Modeling of Slowly Leaking Hydrogen Buoyant Jets in Open Space

Kukhee Lim [a*], Jongtae Kim [b], Yong Jin Cho [a]
[a]*Korea Nuclear Safety Institute, Gwahak-ro 62, Daejeon, Republic of Korea, 34142*
[b]*Korea Atomic Energy Research Institute, Daeduk-daero 989-111, Daejeon, Republic of Korea, 34057*
[*]*Corresponding author: limkh@kins.re.kr*

Keywords : hydrogen, buoyant jet, Froude number, integral equations.

1. Introduction

A hydrogen leak produces a jet that transitions into a plume. This plume, driven by buoyancy, rises quickly, forming a hydrogen-air mixture. These leaks, affected by buoyancy, can be categorized and modeled as slow leaks, as distinct from fast leaks. These leaks can be modeled with entrainment models for turbulent buoyant jets or plumes, assuming appropriate initial conditions for the escaping hydrogen are derived [1,2,3].

This paper aims to model the characteristics of jets from slow hydrogen leaks and validate these models through comparison with experimental data.

2. Modeling

The main assumptions used when modeling a slow leak include [1]:

- The leakage flow is quasi-steady.
- Hydrogen is released at atmospheric pressure.
- Variations in the leak flow's potential and kinetic energy are negligible.
- Heat exchange between the containment and the leak flow stream can be disregarded.

The jet in slow leak is modeled with a series of three turbulent entrainment models as shown in Fig. 1.

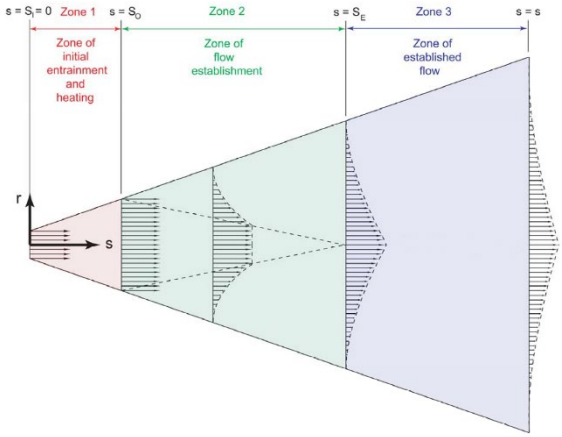

Fig. 1. Flow zones of the slow leak jet model [1]

The pressure in all three zones is assumed to be atmospheric. The model for Zone 2 is used to provide the initial conditions necessary for modeling Zone 3. This model describes how the plug flow of Zone 1 transforms into a fully developed jet flow with Gaussian profiles for both velocity and scalar transport quantities.

In Zone 3, the flow is not considered a plug flow, and the effects of buoyancy are included, which determine the trajectory of the jet or plume. The coordinate system used to describe the jet trajectory and the growth of the jet is illustrated in Fig. 2. The jet axis is aligned along the streamwise coordinate S. The radial coordinate of the jet is r, and the circumferential coordinate of the jet is ϕ. In the overlaid Cartesian coordinate frame of Fig. 2, the angle between the jet axis and the x-axis is θ. Assuming the jet is symmetric about the x-z plane, the relationship between S, θ, x, and z is given as follows:

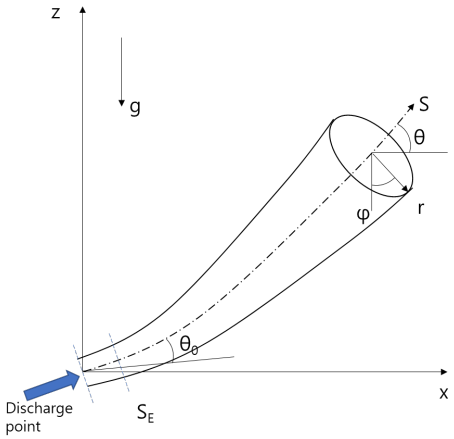

Fig. 2. Flow zones of the slow leak jet model

$$\frac{\partial X}{\partial s} = \cos\theta,\ \frac{\partial Z}{\partial s} = \sin\theta \tag{1}$$

In Zone 3, the integral equations for jet continuity, momentum of the two components, and hydrogen concentration can be summarized as follows:

(Mass conservation):

$$\frac{\partial}{\partial s}\int_0^{2\pi}\int_0^{\infty} \rho u\, r dr d\phi = \rho_\infty E \tag{2}$$

(x-directional momentum conservation):

$$\frac{\partial}{\partial s}\int_0^{2\pi}\int_0^{\infty} \rho u^2 \cos\theta\, r dr d\phi = 0 \tag{3}$$

(z-directional momentum conservation):

$$\frac{\partial}{\partial S}\int_0^{2\pi}\int_0^{\infty}\rho u^2 \sin\theta\, r dr d\phi = \int_0^{2\pi}\int_0^{\infty}(\rho_\infty - \rho)\, g r dr d\phi \quad (4)$$

(Species conservation):

$$\frac{\partial}{\partial S}\int_0^{2\pi}\int_0^{\infty}\rho u(y - y_\infty)\, r dr d\phi = 0 \quad (5)$$

where ρ, u, and y are the jet density, velocity, and hydrogen mass fraction. The subscript ∞ is used to represent the property of the ambient air surrounding the jet. The profiles of the jet properties in Zone 3 are assumed have Gaussian [4,5] and take a form

$$u = u_{cl} e^{-\frac{r^2}{b^2}} \quad (6)$$

$$\rho = \rho_\infty - (\rho_\infty - \rho_{cl}) e^{-\frac{r^2}{\lambda^2 b^2}} \quad (7)$$

$$\rho y = \rho_{cl} y_{cl} e^{-\frac{r^2}{\lambda^2 b^2}} \quad (8)$$

where u_{cl}, ρ_{cl}, and y_{cl} are velocity, density, and hydrogen mass fraction at the centerline. b and λ are the characteristic jet width and the relative radial spreading ratio, respectively. $\lambda = 1.16$ was used here [6]. E is the local rate of entrainment and it is considered to summarize the contribution of momentum, E_{mom}, and buoyancy, E_{buoy}, e.g . [7]

$$E = E_{mom} + E_{buoy} \quad (9)$$

where

$$E_{mom} = 0.282\left(\frac{\pi D_{inlet}^2}{4}\frac{\rho_{inlet} u_{inlet}^2}{\rho_\infty}\right)^{0.5} \quad (10)$$

$$E_{buoy} = \frac{a_2}{Fr_l}(2\pi u_{cl} b)\sin\theta \quad (11)$$

$$a_2 = \begin{cases} 17.313 - 0.11665 Fr_{den} + (2.0771e-4) Fr_{den}^2 & Fr_{den} < 268 \\ 0.97 & Fr_{den} \geq 268 \end{cases} \quad (12)$$

$$Fr_l = \frac{u_{cl}^2}{g D_{inlet}(\rho_\infty - \rho_{cl})/\rho_{inlet}} = \frac{u_{cl}^2 \rho_{inlet}}{g D_{inlet}(\rho_\infty - \rho_{cl})} \quad (13)$$

$$Fr_{den} = \frac{u_0}{\sqrt{gD(\rho_\infty - \rho_o)/\rho_o}} \quad (14)$$

The subscripts "inlet" and "o" represent the characteristics at the inlet and the starting point of Zone 2, respectively. If initial entrainment and heating are absent, allowing Zone 1 to be disregarded, then the characteristics at "inlet" are identical to those with the subscript "o".

After the integration from Equation (2) to (5) by substituting Equation (6) to (8) and rearranging for the derivative terms, the result is as follows:

$$b^2\left[\rho_\infty - (\rho_\infty - \rho_{cl})\left(\frac{\lambda^2}{1+\lambda^2}\right)\right]\frac{\partial u_{cl}}{\partial S} + 2 b u_{cl}\left[\rho_\infty - (\rho_\infty - \rho_{cl})\left(\frac{\lambda^2}{1+\lambda^2}\right)\right]\frac{\partial b}{\partial S} + u_{cl} b^2\left(\frac{\lambda^2}{1+\lambda^2}\right)\frac{\partial \rho_{cl}}{\partial S} = \frac{\rho_\infty E}{\pi} \quad (15)$$

$$\cos\theta b\left[\rho_\infty - (\rho_\infty - \rho_{cl})\left(\frac{2\lambda^2}{1+2\lambda^2}\right)\right]\frac{\partial u_{cl}}{\partial S} + \cos\theta u_{cl}\left[\rho_\infty - (\rho_\infty - \rho_{cl})\left(\frac{2\lambda^2}{1+2\lambda^2}\right)\right]\frac{\partial b}{\partial S} - \frac{\sin\theta}{2} u_{cl} b\left[\rho_\infty - (\rho_\infty - \rho_{cl})\left(\frac{2\lambda^2}{1+2\lambda^2}\right)\right]\frac{\partial \theta}{\partial S} + \frac{\cos\theta u_{cl} b}{2}\left(\frac{2\lambda^2}{1+2\lambda^2}\right)\frac{\partial \rho_{cl}}{\partial S} = 0 \quad (16)$$

$$\sin\theta u_{cl} b\left[\rho_\infty - (\rho_\infty - \rho_{cl})\left(\frac{2\lambda^2}{1+2\lambda^2}\right)\right]\frac{\partial u_{cl}}{\partial S} + \sin\theta u_{cl}^2\left[\rho_\infty - (\rho_\infty - \rho_{cl})\left(\frac{2\lambda^2}{1+2\lambda^2}\right)\right]\frac{\partial b}{\partial S} + \frac{\cos\theta}{2} u_{cl}^2 b\left[\rho_\infty - (\rho_\infty - \rho_{cl})\left(\frac{2\lambda^2}{1+2\lambda^2}\right)\right]\frac{\partial \theta}{\partial S} + \frac{\sin\theta u_{cl}^2 b}{2}\left(\frac{2\lambda^2}{1+2\lambda^2}\right)\frac{\partial \rho_{cl}}{\partial S} = g\lambda^2 b(\rho_\infty - \rho_{cl}) \quad (17)$$

$$b\frac{\partial u_{cl}}{\partial S} + 2u_{cl}\frac{\partial b}{\partial S} - u_{cl} b\left(\frac{RT}{PM_a - RT\rho_{cl}}\right)\frac{\partial \rho_{cl}}{\partial S} = 0 \quad (18)$$

At $s = S_E$, u and b are given by:

$$u_E = u_{cl} \quad (19)$$

$$b_E = \frac{D_o}{\sqrt{\frac{2(2\lambda^2+1)}{\lambda^2\frac{\rho_o}{\rho_\infty} + \lambda^2 + 1}}} \quad (20)$$

Specifically, Eq. (20) is derived from the conservation of mass and momentum from $s = S_O$ to $s = S_E$.

Equation (18) can be obtained by substituting y_{cl} with an expression for ρ_{cl}, derived from the relationship between the ideal gas law and the molecular weight of the mixture. The relationships from Equation (15) to (18) form a set of nonlinear coupled differential equations and can be succinctly organized in the form of a matrix as follows:

$$A\begin{bmatrix}\frac{\partial u_{cl}}{\partial S} \\ \frac{\partial b}{\partial S} \\ \frac{\partial \theta}{\partial S} \\ \frac{\partial \rho_{cl}}{\partial S}\end{bmatrix} = \begin{bmatrix}\frac{\rho_\infty E}{\pi} \\ 0 \\ g\lambda^2 b(\rho_\infty - \rho_{cl}) \\ 0\end{bmatrix} \quad (21)$$

where A represents the matrix that organizes the coefficients of the differential terms in Eq. (15) to (18). To solve Equation (21) for variables u_{cl}, b, θ, and ρ_{cl}, we used Assimulo, a Python module that provides advanced algorithms for solving non-linear differential equations.

3. Validation

For the validation of the program implementing the model, the experiment for a slow leak scenario was based on the small-scale hydrogen slow leak experiments conducted at Sandia National Laboratories [2,8]. The experiment involved hydrogen being jetted vertically (θ = 90º) into free space from a nozzle inlet with D(diameter) = 1.905 mm, under varying flow rates. The temperature and pressure conditions were set at 21 ℃ and 100 kPa, respectively. The flow rate serves as a variable to control the degree of buoyancy effects, and the characteristics of the slow leak flow are defined by Fr_{den} in Equation (14), determined by this variable.

Figs. 3 and 4 illustrate the velocity and density profiles of the jet at various altitudes at Fr_{den} = 268, respectively. As the jet progresses forward (i.e., as S increases in Fig. 2), the analytically implemented model here effectively captures the spreading of the jet in Zone 3, as illustrated in Fig. 1. Fig. 5 illustrates the differences in hydrogen mole fraction profiles at the position of Z/D=100 under various Fr_{den} conditions. The distinction between the two graphs stems from the variation in buoyancy effects, which are determined by the initial velocity of the jet associated with different Fr_{den} values. Specifically, lower Fr_{den} values result in a greater influence of buoyancy, leading to a wider dispersion of the jet, effectively capturing the phenomenon where the jet spreads over a broader area. The influence of buoyancy due to different Fr_{den} conditions is also evident in the comparison of hydrogen mole fraction contours presented in Fig. 6. As the Fr_{den} decreases, it is observed that the jet spreads more extensively, showing smaller mole fractions at smaller values of S, indicating that lower Fr_{den} leads to a more pronounced spreading due to buoyancy effects. Fig. 7 compares the hydrogen mole fraction distribution between experimental and analytical results. While there is a tendency for the jet to spread slightly more narrowly in the analysis compared to the original experimental values, overall, the experimental and analytical results exhibit similar patterns in terms of the jet's spread. When comparing the rising jet in terms of its mole fraction along the centerline, as presented in Fig. 8, it was found to accurately predict the mole fractions for different Fr_{den} conditions. This indicates that the model effectively captures the behavior of the jet's vertical dispersion across various Fr_{den}.

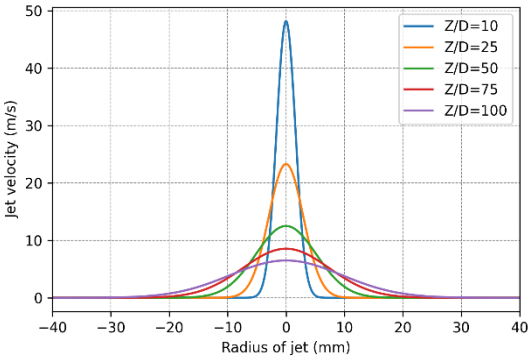

Fig. 3. Jet velocity (Fr_{den}=268)

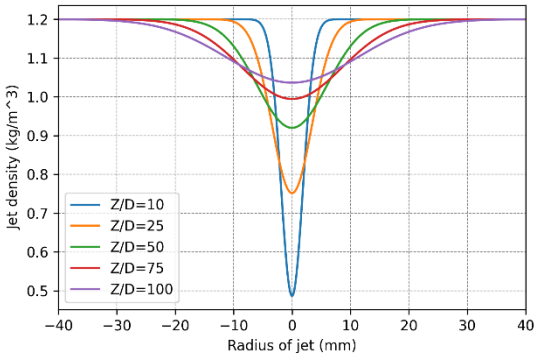

Fig. 4. Jet density (Fr_{den}=268)

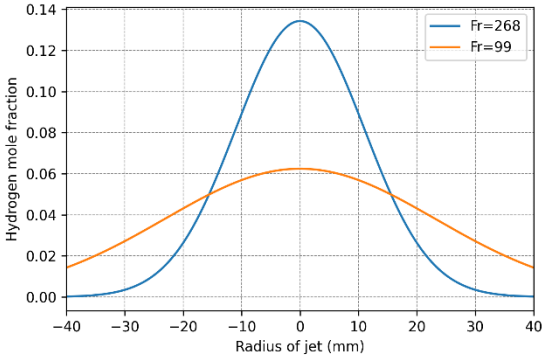

Fig. 5. Comparison of hydrogen mole fraction (Z/D = 100)

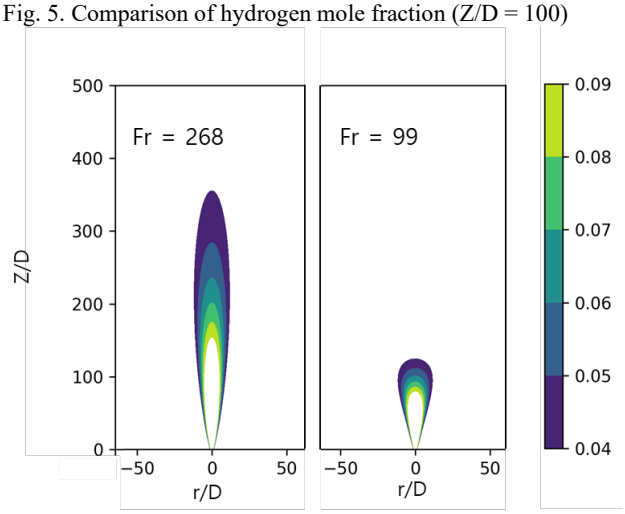

Fig. 6. Hydrogen mole fraction contours

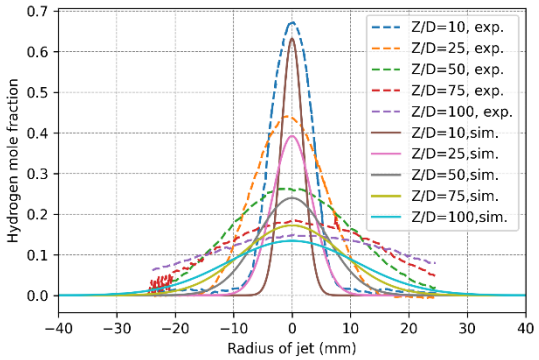

Fig. 7. Hydrogen mole fraction (Fr_{den}=268)

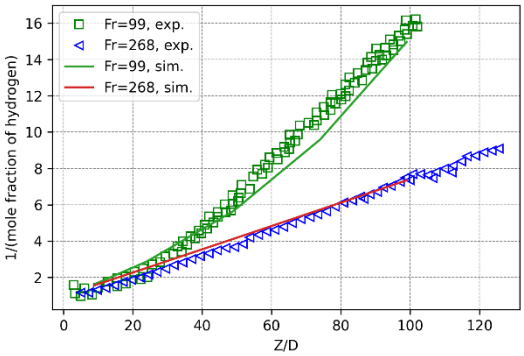

Fig. 8. Comparison of the centerline mole fraction decay

3. Conclusions

In this study, we explored the modeling of slow-leak hydrogen jets in open spaces, particularly focusing on Zone 3 where buoyancy significantly influences jet behavior. Through analytical models and comparison with experimental data, we observed that lower Froude numbers lead to wider jet dispersion due to increased buoyancy effects. While slight discrepancies in jet spread were noted between experimental and analytical results, the overall trends were well captured by the model. This research contributes to a better understanding of hydrogen jet dispersion in the atmosphere, providing insights that are crucial for safety assessments and the development of mitigation strategies in hydrogen technologies. For future work, we aim to compare our model with Computational Fluid Dynamics (CFD) analysis to further validate and refine our predictions. And this technique may be used to utilize the model to reduce analysis time in CFD simulations, such as by predicting the jet profile at various altitudes. This could allow for partial jet modeling with larger mesh sizes, thereby increasing the time step size and reducing computational time. These steps are anticipated to enhance the efficiency and applicability of hydrogen jet modeling in practical scenarios.

ACKNOWLEDGEMENT

This work was supported by the Nuclear Safety Research Program through the Korea Foundation Of Nuclear Safety(KoFONS) using the financial resource granted by the Nuclear Safety and Security Commission(NSSC) of the Republic of Korea. (No. 2106007).

REFERENCES

[1] W. S. Winters, “Modeling Leaks from Liquid Hydrogen Storage Systems”, Sandia National Laboratories, SAND2009-0035, 2009.
[2] W. Houf, and R. Schefer, Analytical and experimental investigation of small-scale unintended release of hydrogen, International Journal of Hydrogen Energy, Vol. 33, p. 1435, 2008.
[3] David M. Christopher, BI Jingliang, and LI Xuefang, Integral model and CFD simulations for hydrogen leaks, Huagong Xuebao/CIESC Journal. Vol. 64. P. 3088, 2013 (in Chinese).
[4] W. M. Pitts, Effects of global density ratio on the centerline mixing behavior of axisymmetric turbulent jets, Experiments in Fluids, Vol. 11, p. 125, 1991.
[5] W.R. Keagy, and A.E. Weller, A study of freely expanding inhomogeneous jets, Proc. Heat Transfer and Fluid Mechanics Institute, p. 8. 1949.
[6] Benjamin G., David S. H., and Matthew K., The Diffusion of Turbulent Buoyant Jets, Advances in Heat Transfer, Vol. 16, p.1, 1984.
[7] Hirst EA. Analysis of buoyant jets within the zone of flow establishment, Oak Ridge National Laboratory, ORNL-TM-3470, 1971.
[8] R.W. Schefer, W.G. Houf, T.C. Williams, Investigation of small-scale unintended releases of hydrogen: Buoyancy effects, International Journal of hydrogen energy, Vol. 33, p. 4702, 2008.